



Research article

Role of microRNA-520h in 20(R)-ginsenoside-Rg3-mediated angiosuppression



Man-Hong Keung¹, Lai-Sheung Chan¹, Hoi-Hin Kwok^{1,2}, Ricky Ngok-Shun Wong^{1,2,*}, Patrick Ying-Kit Yue^{1,2,**}

¹ Department of Biology, Faculty of Science, Hong Kong Baptist University, Hong Kong Special Administrative Region

² Dr. Gilbert Hung Ginseng Laboratory, Hong Kong Baptist University, Hong Kong Special Administrative Region

ARTICLE INFO

Article history:

Received 4 May 2015

Received in Revised form

30 June 2015

Accepted 10 July 2015

Available online 29 July 2015

Keywords:

anti-angiogenesis

ginsenoside-Rg3

microRNA

miR-520h

ABSTRACT

Background: Ginsenoside-Rg3, the pharmacologically active component of red ginseng, has been found to inhibit tumor growth, invasion, metastasis, and angiogenesis in various cancer models. Previously, we found that 20(R)-ginsenoside-Rg3 (Rg3) could inhibit angiogenesis. Since microRNAs (miRNAs) have been shown to affect many biological processes, they might play an important role in ginsenoside-mediated angiomodulation.

Methods: In this study, we examined the underlying mechanisms of Rg3-induced angiosuppression through modulating the miRNA expression. In the miRNA-expression profiling analysis, six miRNAs and three miRNAs were found to be up- or down-regulated in vascular-endothelial-growth-factor-induced human-umbilical-vein endothelial cells (HUVECs) after Rg3 treatment, respectively.

Results: A computational prediction suggested that mature hsa-miR-520h (miR-520h) targets ephrin receptor (Eph) B2 and EphB4, and hence, affecting angiogenesis. The up-regulation of miR-520h after Rg3 treatment was validated by quantitative real-time polymerase chain reaction, while the protein expressions of EphB2 and EphB4 were found to decrease, respectively. The mimics and inhibitors of miR-520h were transfected into HUVECs and injected into zebra-fish embryos. The results showed that overexpression of miR-520h could significantly suppress the EphB2 and EphB4 protein expression, proliferation, and tubulogenesis of HUVECs, and the subintestinal-vessel formation of the zebra fish.

Conclusion: These results might provide further information on the mechanism of Rg3-induced angiosuppression and the involvement of miRNAs in angiogenesis.

Copyright 2015, The Korean Society of Ginseng, Published by Elsevier. This is an open access article under the CC BY-NC-ND license (<http://creativecommons.org/licenses/by-nc-nd/4.0/>).

1. Introduction

Panax ginseng Meyer has been applied as general “tonic” and therapeutics for many years in Asian countries. Its diverse pharmacological activities are largely attributed to ginsenosides, the major active component found in ginseng. Among the ginsenosides, 20(R)-ginsenoside-Rg3 (Rg3) (Fig. 1), a partially deglycosylated saponin that presents in relatively large quantity in red ginseng, has been shown as a potent angiosuppressive and anti-tumor agent [1–3]. Our previous findings demonstrated that Rg3 could suppress human-umbilical-vein-endothelial-cell (HUVEC) proliferation, tubulogenesis, and vascular-endothelial-growth-

factor (VEGF)-induced chemoinvasion; *in vivo* neovessel formation in a Matrigel plug model; and endothelial sprouting and matrix-metalloproteinase production in cultured aortic explants [3]. Moreover, it has been shown that the combined application of Rg3 with different conventional chemotherapeutic drugs, including capecitabine, cyclophosphamide, or gemcitabine, could significantly inhibit the intratumoral microvessel formation of tumor tissues in mice implanted with breast or lung carcinoma [4–8].

However, it has been well accepted that VEGF plays a critical role in tumor progression, metastasis, as well as angiogenesis. A large amount of VEGF is being produced by the hypoxic tumor tissues to

* Corresponding author. Room SCT1116, Science Tower, Hong Kong Baptist University, Hong Kong

** Corresponding author. Room SCT1004A, Science Tower, Hong Kong Baptist University, Hong Kong

E-mail addresses: rns Wong@hkbu.edu.hk (R.N.-S. Wong), Patrick@hkbu.edu.hk (P.Y.-K. Yue).

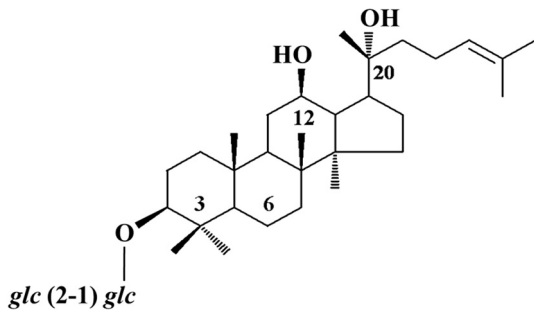


Fig. 1. The chemical structure of 20(R)-ginsenoside Rg3.

initiate angiogenesis in order to feed the growing tumor. Data also showed that Rg3 could significantly inhibit VEGF and VEGF receptor expression in HUVECs, tumor tissues, and animal sera of tumor-bearing mice [9]. To this end, we employed this VEGF-mediated angiogenesis model in our angiosuppressive studies, in which HUVECs were induced with VEGF to mimic the tumor microenvironment. Obviously, Rg3 was found to exhibit a more significant angiosuppressive effect in the VEGF-activated HUVECs. In the present study, in order to investigate the microRNA (miRNAs)-mediated angiosuppressive mechanism of Rg3, the miRNA-expression profile was determined in the VEGF-activated HUVECs upon Rg3 treatment.

A growing body of evidence indicates that miRNAs, a group of small noncoding RNAs that regulate gene expression post-transcriptionally, play an important role in regulating diverse cellular processes, such as proliferation, differentiation, cell cycle, and apoptosis [10,11]. They have also been suggested as molecular determinants of many physiological and pathological processes [12,13]. Previously, we have extended our ginseng pharmacological studies to the miRNA-mediated biochemical pathways. We showed that ginsenoside Rg1-induced angiogenesis could be mediated by a group of miRNAs as determined by a microarray-based miRNA experiment, in which down-regulated miR-214 and miR-15b were found to correlate with the increased production of angiogenic factor, endothelial nitric oxide synthase [14], and angiogenic receptor, VEGF receptor 2 (VEGFR-2) [15], in HUVECs. These data strongly indicated that miRNAs play an important role in ginsenoside-mediated angiomodulation. Therefore, we speculated that Rg3 may also modulate the miRNA expression that leads to inhibit angiogenesis.

In the present study, a miRNA-expression profiling analysis was performed to select the miRNA candidates involved in the Rg3-induced angiosuppression. Again, gain-of-function and loss-of-function experiments were used to investigate the functional roles of the target miRNAs.

2. Materials and methods

2.1. Chemicals

Rg3 (Fig. 1) is a reference compound (purity > 98%) purchased from the Division of Chinese Materia Medica and Natural Products, National Institute for the Control of Pharmaceutical and Biological Products, Ministry of Public Health, China. A stock solution of 20(R)-Rg3 at 50mM was prepared in dimethyl sulfoxide.

2.2. Cell culture

HUVECs (Lonza, Allendale, NJ, USA) were grown in M199 medium supplemented with 20 µg/mL endothelial-cell-growth supplement,

90 µg/mL heparin (Sigma, Saint Louis, MO, US), 20% heat-inactivated fetal bovine serum (HI-FBS), and 1% penicillin–streptomycin (Invitrogen, Boston, MA, USA) on 0.1% gelatin-coated culture flasks. The cells were grown at 37°C in a humidified incubator with 5% CO₂. HUVECs from passages 2–6 were used in this study.

2.3. The miRNA-microarray analysis [14]

2.3.1. Small RNA isolation

VEGF-induced HUVECs were treated with 100nM Rg3 in M199 supplemented with 10% HI-FBS for 24 h. The control experiment was set up in parallel by culturing HUVECs without Rg3. Total RNA was extracted using the TRIzol Reagent (Invitrogen); the quantity and integrity of the RNA preparation were assessed by measuring optical density at 260 nm using the NanoDrop ND-1000 Spectrophotometer (NanoDrop Technologies, Wilmington, DE, USA) and agarose gel electrophoresis, respectively. The small RNA was purified and enriched through a column-based method using the PureLink miRNA Isolation Kit (Invitrogen).

2.3.2. The miRNA labeling and microarray hybridization

Small cellular RNAs extracted from the VEGF-induced HUVECs (control) and the Rg3-treated VEGF-induced HUVECs (treatment) were polyadenylated at the 3'-end by NCode miRNA Labeling System (Invitrogen), and ligated with capture sequences in Alexa Fluor 5 Ligation Mix or Alexa Fluor 3 Ligation Mix separately. The tagged miRNA was purified by spin-column-based centrifugation, and immediately hybridized with miRNA microarray (NCode Multi-Species miRNA Microarray Kit V2, Invitrogen) at 52°C for 16 h. After hybridization, the microarray slides were washed and spin dried, and subsequently labeled with Alexa Fluor 3 and Alexa Fluor 5 correspondingly in the dark at 62°C for 4 h. The slides were washed and spin dried before scanning.

2.3.3. Microarray imaging and data analysis

The miRNA microarrays were screened using the ScanArray 5000 confocal laser scanner (Packard BioChip Technologies/GSI Lumonics) at 556 nm and 650 nm for Alexa Fluor 3 and Alexa Fluor 5, respectively. The fluorescent signals of Alexa Fluor 3 and 5 on each spot were quantified by QuantArray quantitative microarray analysis software (GSI Lumonics). Using GeneSpring GX software (version 10.0; Agilent Technologies, Palo Alto, CA, USA), the spot signals were further analyzed and normalized by locally weighted regression scatterplot smoothing, where 20% of the data were used for smoothing and the cutoff value was 10.0. The miRNA expression was considered down- or up-regulated if the fold change in expression level (Rg3 + VEGF/VEGF) was ≤ -2 or ≥ 2 , respectively.

2.4. Transient transfection with miRNA inhibitor or precursor mimics

HUVECs were transfected with Pre-miR miRNA Precursor (Pre-miR-520h) or Anti-miR miRNA Inhibitor (AS-miR-520h) (20nM) (Ambion, Grand Island, NY, USA) using Lipofectamine 2000 in Opti-MEM I Reduced Serum Medium (Invitrogen). Pre-miR miRNA Precursor Negative Control #1 (precontrol) and Anti-miR miRNA Inhibitor Negative Control #1 (AS-control) (Ambion) were used as negative controls in the experiments involving Pre-miR miRNA Precursor and Anti-miR miRNA Inhibitor, respectively. The total RNA and cell lysate were collected for the indicated assays.

2.5. Quantitative real-time polymerase chain reaction

The total RNA (10 ng) extracted from the cells was converted to complementary DNA (cDNA) using TaqMan MicroRNA Reverse

Transcription Kit and miRNA-specific loop reverse transcription (RT) primer (5×) from TaqMan MicroRNA Assays (Applied Biosystems, Foster City, CA, USA). Real-time polymerase-chain-reaction (PCR) amplification was performed by Bio-Rad iCycler, version 4.006 (Bio-Rad Laboratories, Wilmington, North Carolina, USA) using TaqMan 2× Universal PCR Master Mix (No AmpErase UNG) and TaqMan Assay (20×) from TaqMan MicroRNA Assays (Applied Biosystems). The data were analyzed by iCycler iQ Optical System Software, version 3.0a (Bio-Rad Laboratories). The relative level of mature hsa-miR-520h (miR-520h) in HUVECs was calculated against U6 RNA (internal control) using the $2^{-\Delta\Delta C_t}$ method. The PCRs were run along with the no-template and RT-minus controls.

2.6. Western blot analysis

Equal amounts of protein samples (20 µg) extracted from the cells were resolved using 12% sodium dodecyl sulfate–polyacrylamide gel electrophoresis under a reducing condition, and subsequently transferred onto a nitrocellulose membrane. After blotting, the membrane was probed with primary antibodies against anti-ephrin receptor (Eph) B2, anti-EphB4 (R&D Systems, MIT, Boston, USA), and actin (Sigma), and followed by an incubation with a secondary antibody. The membrane was then washed and visualized by ECL detection system (Bio-Rad Laboratories). Actin expression was used as protein loading control. Densitometry quantification was performed in ImageJ software (<http://rsb.onio.nih.gov>). At least three independent experiments were carried out to study the protein expression.

2.7. In vitro proliferation assay

HUVECs (4×10^4 cells/well) with or without transfection of Pre-miR-520h or AS-miR-520h oligonucleotide were seeded onto 96-well gelatin-coated plates at a density of 1×10^4 cells/well. The cells were allowed to grow for 48 h in M199 with 10% HI-FBS at 37°C. The metabolic activity was analyzed after the addition of 20 µL of 3-(4,5-Dimethylthiazol-2-yl)-2,5-Diphenyltetrazolium Bromide (MTT) for 4 h. The formation of a purple formazan solution was measured at 540 nm and 690 nm.

2.8. In vitro tube-formation assay

HUVECs (2×10^4 cells/well) with or without transfection of Pre-miR-520h or AS-miR-520h oligonucleotide were plated onto a 96-well plate coated with growth-factor-reduced Matrigel (BD Biosciences, Billerica, MA, USA), and incubated at 37°C for 8 h. The tubes that formed in each well were captured using a stereomicroscope (Olympus SZX16) with an attached digital camera (Olympus DP71). The branch points of the tubes that formed in each well were counted, and the averaged numbers of the branch points were calculated. Three independent experiments were performed, and each experiment was run in triplicates.

2.9. In vivo zebra-fish angiogenesis assay

2.9.1. Maintenance of zebra fish and collection of embryos

Wild-type zebra fish were obtained from a local supplier, and were maintained and bred as described in our previous publication [16]. The zebra fish were maintained on a 14 h:10 h light/dark cycle at 28°C, and were fed twice daily with tropical fish food. Embryos were generated by natural pair-wise mating when the fish were mature (6 months old or above). To prepare for mating, the breeding tank was submerged into the fish tank just before switching on the light in the morning. After 2 h, the embryos were harvested and transferred to Petri dishes containing fresh water. All

the animal experiments were approved by the animal ethics committee of the Hong Kong Baptist University. The procedures were reported according to the Animal Research: Reporting *In Vivo* Experiments guidelines. All procedures performed were meant to minimize the number of use and suffering of the animals.

2.9.2. Microinjection

Fertilized one- to four-cell-stage zebra-fish embryos were injected with 1 µL of 10µM miRNA inhibitor or miRNA precursor (Ambion). Pre-miR miRNA Precursor Negative Control #1 (Pre-NC; Ambion) and Anti-miR miRNA Inhibitor Negative Control #1 (Anti-NC; Ambion) were used as negative controls in this experiment. The injected embryos were incubated in embryo water (0.2 g/L of Instant Ocean salt in distilled water) with 0.003% 1-phenyl-2-thiourea at 28.5°C. At least 30 embryos were analyzed in each experimental condition.

2.9.3. Endogenous alkaline-phosphatase-based vascular staining

After 3 days of incubation (3 days postfertilization), the embryos were euthanized, and alkaline-phosphatase activity was assayed after overnight fixation at 4°C in 4% paraformaldehyde. The endogenous melanin in the fish-embryo pigment cells was removed by incubating in 1% KOH and 3% H₂O₂ for 20 min, followed by 0.1% phosphate-buffered saline in Tween 20 (PBST) rinsing. Then, fish embryos were treated with precooled acetone for 30 min at –20°C and rinsed with PBST. For staining, the embryos were equilibrated with NTMT buffer (100mM Tris with pH 9.7, 50mM MgCl₂, 100mM NaCl, and 0.1% Tween 20) at room temperature, and subsequently stained with nitroblue tetrazolium/5-bromo-4-chloro-3-indolyl-phosphate (AMRESCO, Solon, OH, USA) at room temperature in the dark. Finally, the fish embryos were fixed again in 4% paraformaldehyde followed by PBST rinsing. The subintestinal-vessel (SIV) basket of the stained zebra fish was examined under the stereomicroscope (Olympus SZX16) with an attached digital camera (Olympus DP71) (Olympus America, Inc.). Areas of the SIVs were quantified by the ImageJ software.

2.10. 3'-UTR luciferase-reporter assay

Luciferase-reporter vectors containing 3'-UTR of EphB2 and EphB4 were purchased from SwitchGear Genomics, Menlo Park, CA,

Table 1

Differentially expressed microRNAs after 20(R)-ginsenoside-Rg3 treatment in vascular-endothelial-growth-factor-induced human umbilical vein endothelial cells

| Mature miRNAs | Mature miRNA sequence (5'–3') | miRBase accession number | Fold change (VEGF + Rg3/VEGF) |
|-----------------------------|-------------------------------|--------------------------|-------------------------------|
| Up-regulated miRNAs | | | |
| hsa-miR-520h | acaagugcuuccuuuagagu | MIMAT0002867 | 15.32 ± 3.9 |
| hsa-miR-487b | aaucguacagggucauccacuu | MIMAT0003180 | 10.10 ± 4.29 |
| hsa-miR-197 | uucaccacuuuccaccaccagc | MIMAT0000227 | 6.89 ± 2.28 |
| hsa-miR-524* | cuacaaaggaagcacuucuc | MIMAT0002849 | 3.02 ± 1.01 |
| hsa-miR-342 | ucucacacagaaucgcccgc | MIMAT0000753 | 2.58 ± 0.85 |
| hsa-miR-219 | ugauuguccaaacgcauuuc | MIMAT0000276 | 2.26 ± 0.7 |
| Downregulated miRNAs | | | |
| hsa-miR-23a | aucacauugccagggaauuucc | MIMAT0000078 | –3.81 ± 1.94 |
| hsa-miR-489 | gugacacacauaucggcagc | MIMAT0002805 | –4.95 ± 2.56 |
| hsa-miR-377 | aucacacaaaggcauuuuuu | MIMAT0000730 | –34.94 ± 15.03 |

VEGF-induced HUVECs were treated with or without Rg3 (100nM) for 24 h. Extracted small RNAs were fluorescently labeled with Alexa Fluor 5 or 3, and hybridized onto miRNA microarray. The miRNA expression was considered up- or downregulated if the fold change in the expression level detected in Rg3-treated group (Rg3 + VEGF) versus control group (VEGF alone) was over 2 or below –2, respectively. Three individual experiments were performed, and each miRNA was spotted on the microarray chip in triplicate. Values of fold change are presented as mean ± standard error of the mean
HUVEC, human umbilical vein endothelial cell; miRNA, microRNA; VEGF, vascular endothelial growth factor

USA. To confirm the putative binding site, the seed regions of miR-520h on EphB2 and EphB4 3'-UTR were converted to consecutive cytosine using QuikChange Lightning Multi Site-Directed Mutagenesis Kit (Agilent Technologies). Mutation was confirmed by DNA sequencing. COS-7 was cultured in Dulbecco's modified Eagle's medium with 10% fetal bovine serum. Cells seeded onto a 96-well plate (3×10^4 cells/well) were cotransfected with the reporter vector (50 ng) and miRNA synthetic oligonucleotides (50nM) by Lipofectamine 2000. After 24 h of transfection, the cell lysate was harvested, and luciferase activity was detected using Luciferase Assay System (Promega, Madison, WI, USA) with a microplate luminometer (Infinite F200; Tecan, Männedorf, Switzerland). The luminescence reading was normalized by protein content in each well.

2.11. Statistical analysis

Data were presented as mean \pm standard deviation (SD) unless otherwise specified. Statistical comparisons between two groups

were carried out by the Student *t* test or one-way analysis of variance (SigmaPlot version 12.5). The statistical significance was set as $p < 0.05$.

3. Results

3.1. The miRNA-expression profiling of Rg3-treated VEGF-induced HUVECs

As shown in Table 1, among the screened 553 human miRNAs, nine miRNAs were found to differentially express in VEGF-induced HUVECs after Rg3 treatment. Among them, both miR-520h and miR-487b increased more than 10-fold, while four other miRNAs including miR-219, miR-342, miR-524*, and miR-197, were up-regulated from 2.36 to 6.89 folds. Besides, three miRNAs, including miR-23a, miR-489, and miR-377, were differentially down-regulated in the range of 3.81–34.94 folds. The microarray data have been deposited in the Gene Expression Omnibus public database with

A EPHB2 and EPHB4 mRNA

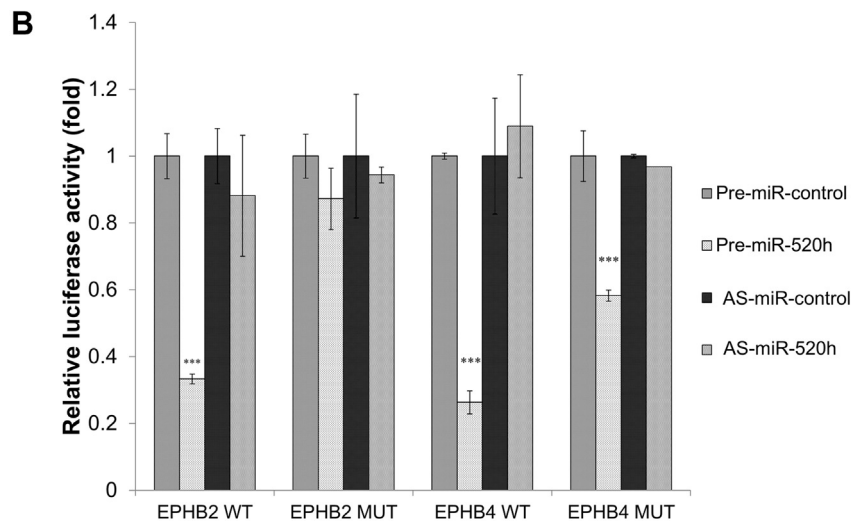
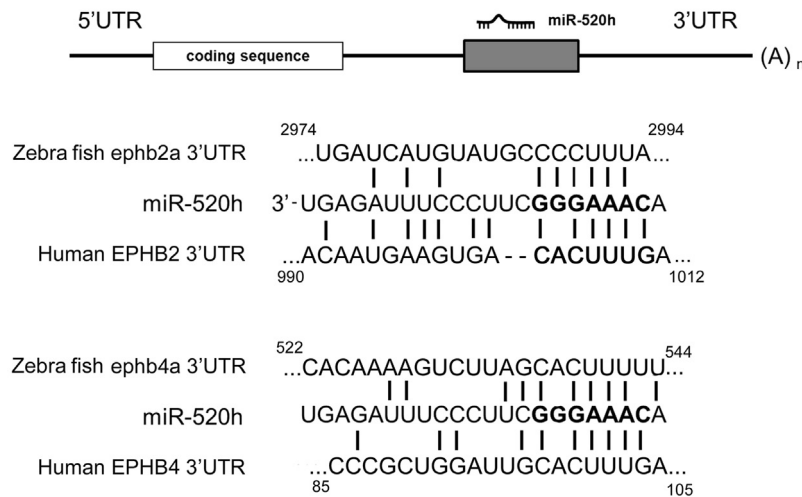


Fig. 2. The mature hsa-miR-520h (miR-520h) targets on ephrin receptor (Eph) B2 and EphB4 3'-UTR. (A) The computational target prediction of TargetScan suggested that miR-520h is partially complementary to the RNA sequence within the EphB2 and EphB4 3'-UTR. (B) Luciferase-reporter plasmid bearing wild-type (WT) or mutated (MUT) EphB2 and EphB4 messenger RNA 3'-UTR was cotransfected with miR-520h precursor or inhibitor (50nM) for 24 h in COS-7. Values are presented as means \pm standard deviation. Asterisks denote a significant difference compared with the values for the precontrol. *** $p < 0.001$.

series record number GSE31959 (<http://www.ncbi.nlm.nih.gov/geo/info/linking.html>).

3.2. Bioinformatics prediction of potential gene targets of miR-520h

Among the nine miRNA candidates, miR-520h showed the highest up-regulated level and consistency; it was selected as the investigation target in this study. Using an online database for miRNA target prediction (release 6.2: June 2012; <http://www.targetscan.org/>), miR-520h is found to be partially complementary to the RNA sequence extending from nucleotide 990 to 1012 within EphB2 3'-UTR, and the sequence extending from nucleotide 85 to 105 within EphB4 3'-UTR (Fig. 2A). While ephrin is closely related to cell migration and angiogenesis, we believed that EphB2 and EphB4 might be the target of miR-520h in Rg3-induced anti-angiogenesis. To further confirm the interaction of miR-520h on EphB2 and EphB4 3'-UTR, luciferase-reporter vectors containing the full length of EphB2 or EphB4 messenger RNA (mRNA) 3'-UTR were cotransfected with miRNA precursor mimics (Pre-miR-520h) or antisense miR-520h (AS-miR-520h) into COS-7. From Fig. 2B, overexpression of miR-520h could significantly inhibit EphB2 and EphB4 3'-UTR luciferase activities for about 60%, while the transfection of miR-520h inhibitor showed no significant effects. Mutation of the putative seed region of EphB2 mRNA 3'-UTR could completely abolish the inhibition by overexpression of miR-520h. However, similar mutation on EphB4 mRNA 3'-UTR could only partially reduce the inhibition by miR-520h, which indicated that there may be another unidentified binding site on the 3'-UTR. Otherwise, miR-520h may target on regulator upstream of EphB4, thus providing an indirect effect.

3.3. Validation of miR-520h expression and potential gene targets

To confirm the overexpression of miR-520h in Rg3-treated endothelial cells, real-time PCR was performed. Using U6 as internal control, the ratio of miR-520h to U6 RNA in the control cells was arbitrarily set at 1. The results showed that the relative expression of miR-520h was found to increase by 2.98-fold in HUVECs upon the Rg3 treatment (Fig. 3), which is concomitant to our microarray-

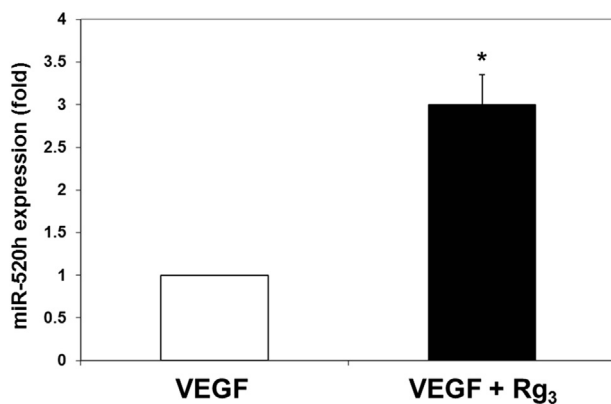


Fig. 3. 20(R)-ginsenoside-Rg3 (Rg3) increases the mature hsa-miR-520h (miR-520h) expression in vascular-endothelial-growth-factor (VEGF)-induced human-umbilical-vein endothelial cells. The expression level of miR-520h in VEGF-induced human-umbilical-vein endothelial cells upon Rg3 treatment was measured using quantitative real-time polymerase chain reaction. The cells were cultured in M199 medium supplemented with 10% heat-inactivated fetal bovine serum and 25 ng/mL VEGF, with or without Rg3 for 24 h. The relative expression of miR-520h was calculated against U6 RNA with the $2^{-\Delta\Delta Ct}$ method. All polymerase chain reactions were run in triplicates in at least three independent experiments. Values are presented as means \pm standard deviation. The asterisk denotes a significant difference compared with the values for the corresponding control. * $p < 0.05$.

profiling data. Besides, the expression levels of EphB2 and EphB4, which are the potential targets of miR-520h, were measured by Western blotting analysis. As shown in Fig. 4, the expression level of EphB2 was almost completely suppressed, while B4 was decreased by 2.3-fold in Rg3-treated HUVECs.

3.4. Functional roles of miR-520h in angiogenesis

In order to demonstrate the roles of miR-520h in Rg3-induced angiogenesis, expression levels of target proteins EphB2 and EphB4, tube formation and proliferation ability of HUVECs, and SIV formation of zebra-fish embryos were measured after the introduction of Pre-miR-520h or AS-miR-520h transfection or microinjection. As shown in Fig. 5A, when HUVECs were transfected with Pre-miR-520h, the level of miR-520h was greatly increased, as measured by quantitative real-time PCR (qRT-PCR) analysis. The Western blotting analysis indicated that the expression of the target protein EphB2 was reduced in about 20%, while EphB4 was totally diminished when compared with the control group (Fig. 5B). Moreover, the functional role of miR-520h was clearly demonstrated in various bioassays. In Fig. 5C and 5D, overexpression of miR-520h was found to significantly suppress HUVEC proliferation and tubulogenesis in about 18% and 35%, respectively. Finally, the *in vivo* angiogenesis model was employed, and precursor mimics of miR-520h were injected into the zebra-fish embryos. Data showed that the neovessel formation in the SIV basket was significantly suppressed in the presence of miR-520h when compared with the precontrol group (Fig. 5E). These results suggested that miR-520h might be important in angiogenesis through modulating EphB2 and EphB4. Conversely, experiments were repeated by transfecting an antagomiR antisense (AS-miR-520h) to mature miR-520h. With reference to the internal U6 RNA expression, transfection of AS-

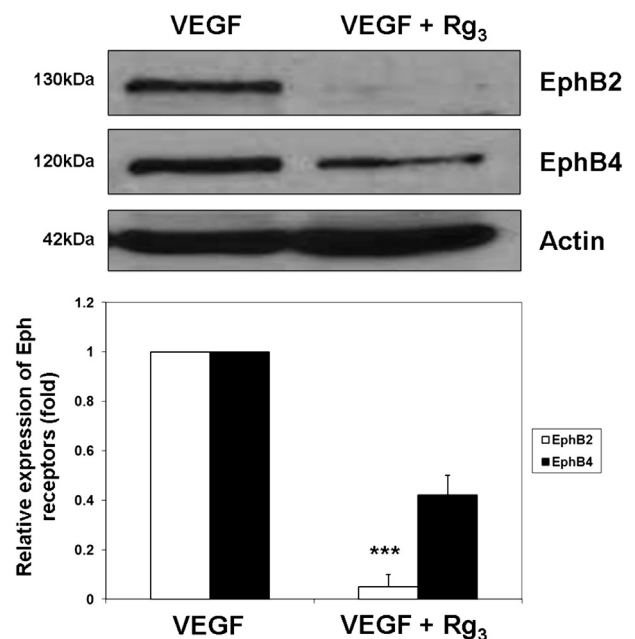


Fig. 4. 20(R)-ginsenoside-Rg3 (Rg3) suppresses ephrin receptor (Eph) B2 and EphB4 expression in vascular-endothelial-growth-factor (VEGF)-induced human-umbilical-vein endothelial cells. Total protein was harvested from treatment (VEGF + Rg3) and control (VEGF) group cells. Then, the expression levels of EphB2 and EphB4 were analyzed by Western blotting with indicated antibodies (upper panel). The relative expressions of EphB2 and EphB4 were normalized and quantified against actin (lower panel). Values are presented as means \pm standard deviation of three independent experiments. Asterisks denote a significant difference compared with the values for the corresponding control. ** $p < 0.01$; *** $p < 0.001$.

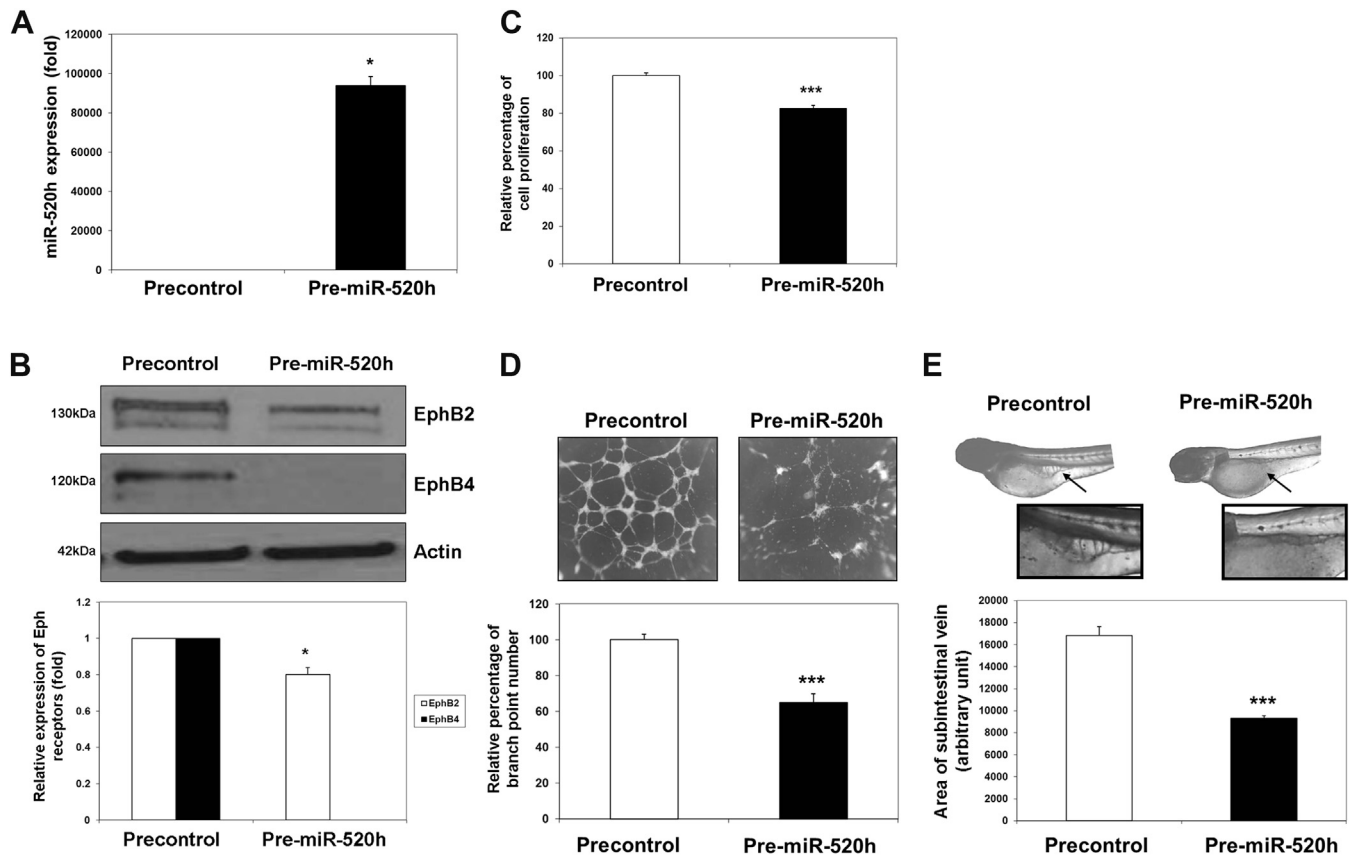


Fig. 5. Elevated level of the mature hsa-miR-520h (miR-520h) diminishes ephrin receptor (Eph) B2 and EphB4 expression, human-umbilical-vein-endothelial-cell (HUVEC) proliferation and tubulogenesis, and zebra-fish subintestinal-vessel (SIV) formation. (A) Transfection of Pre-miR-520h oligonucleotide (20nM) for 24 h significantly elevated the miR-520h level in HUVECs. The miR-520h level was quantitated by quantitative real-time polymerase chain reaction. Three independent experiments were performed, and each experiment was in three replicates. (B) Increased level of miR-520h suppressed EphB2 and EphB4 expressions in HUVECs. Total protein was harvested from Pre-miR-520h or precontrol transfected HUVECs, and EphB2 and EphB4 expression levels were measured by Western blotting (upper panel), and quantified with actin normalization (lower panel). (C) and (D) Transfection of Pre-miR-520h oligonucleotide suppressed HUVEC proliferation and tubulogenesis. Upon transfection, HUVECs were cultured for 48 h, and growth inhibition was determined by 3-(4,5-Dimethylthiazol-2-yl)-2,5-Diphenyltetrazolium Bromide (MTT) assay. Tubulogenesis was measured by counting the number of branch points formed by HUVECs on the Matrigel. Three independent experiments were performed, and each experiment was in four replicates. (E) Microinjection of Pre-miR-520h into zebra-fish embryo greatly inhibited the SIV basket formation. Photomicrographs depict SIV formation in 3 days postfertilization fish embryo in defined condition. The area of the SIV basket was measured by ImageJ software. Values are presented as means \pm standard deviation. Asterisks denote a significant difference compared with the values for the corresponding control. * $p < 0.05$, ** $p < 0.01$, *** $p < 0.001$.

miR-520h significantly reduced the endogenous miR-520h level in HUVECs when compared with the AS-control group (Fig. 6A). Subsequently, as we expected, the EphB2 and EphB4 expression levels should be affected to a certain extent. However, it was found that the EphB2 and EphB4 expression levels in HUVECs were not much increased upon AS-miR-520h transfection (Fig. 6B). Similar results were observed in both *in vitro* and *in vivo* angiogenic assays, in which there were no measurable changes in HUVEC proliferation and tube formation (Fig. 6C and 6D), as well as in the zebra-fish SIV formation assay (Fig. 6E). To show the inhibitory effect of Rg3 on angiogenesis, which is indeed mediated through the induction of miR-520h, HUVECs were first transfected with AS-control or AS-miR-520h, and then VEGF and Rg3 were added to the cells. The inhibitory effects of Rg3 on HUVEC proliferation (Fig. 7A) and tubulogenesis (Fig. 7B) were both abolished by the transfection of AS-miR-520h, which indicated that the increase of expression of miR-520h is essential to its angioppressive effects.

4. Discussion

The anti-angiogenic strategy of cancer therapy has been proposed for more than 40 years, and the first anti-angiogenic drug, Avastin (bevacizumab), was approved by the US Food and Drug

Administration in 2004 for cancer treatment [17]. As predicted, the focus has been directed toward discovering more novel anti-angiogenic agents, such as TNP-470 and thalidomide. As ginsenoside-Rg3 has been packaged as “Shenyi jiaonang” in mainland China and used for cancer treatment, its pharmacological mechanisms are still unclear. In this study, we tried to investigate how Rg3 could inhibit angiogenesis through modulating the miRNA expression. Data showed that Rg3 could modulate a series of miRNA expressions in the VEGF-induced HUVECs, whereas miR-520h was selected from the microarray-based screening for a detailed study, as it is the most differentially expressed with a higher degree of consistency.

In fact, there is not much research about miR-520h in the literature; until recent years, the anticancer activity of miR-520h was proposed. It has been suggested as a specific marker for a better classification of oral squamous cell carcinoma, and differentiation of pathologic pregnancies [18,19]. Moreover, Su et al [20] have provided clinical data about the significance of miR-520h in lung-cancer patients. They demonstrated the possible link between resveratrol-mediated miR-520h expression and lung-cancer migration and invasion abilities. They also showed that miR-520h was critical for adenoviral oncogene-mediated antimetastatic lung-colony formation in an experimental metastasis and lung-

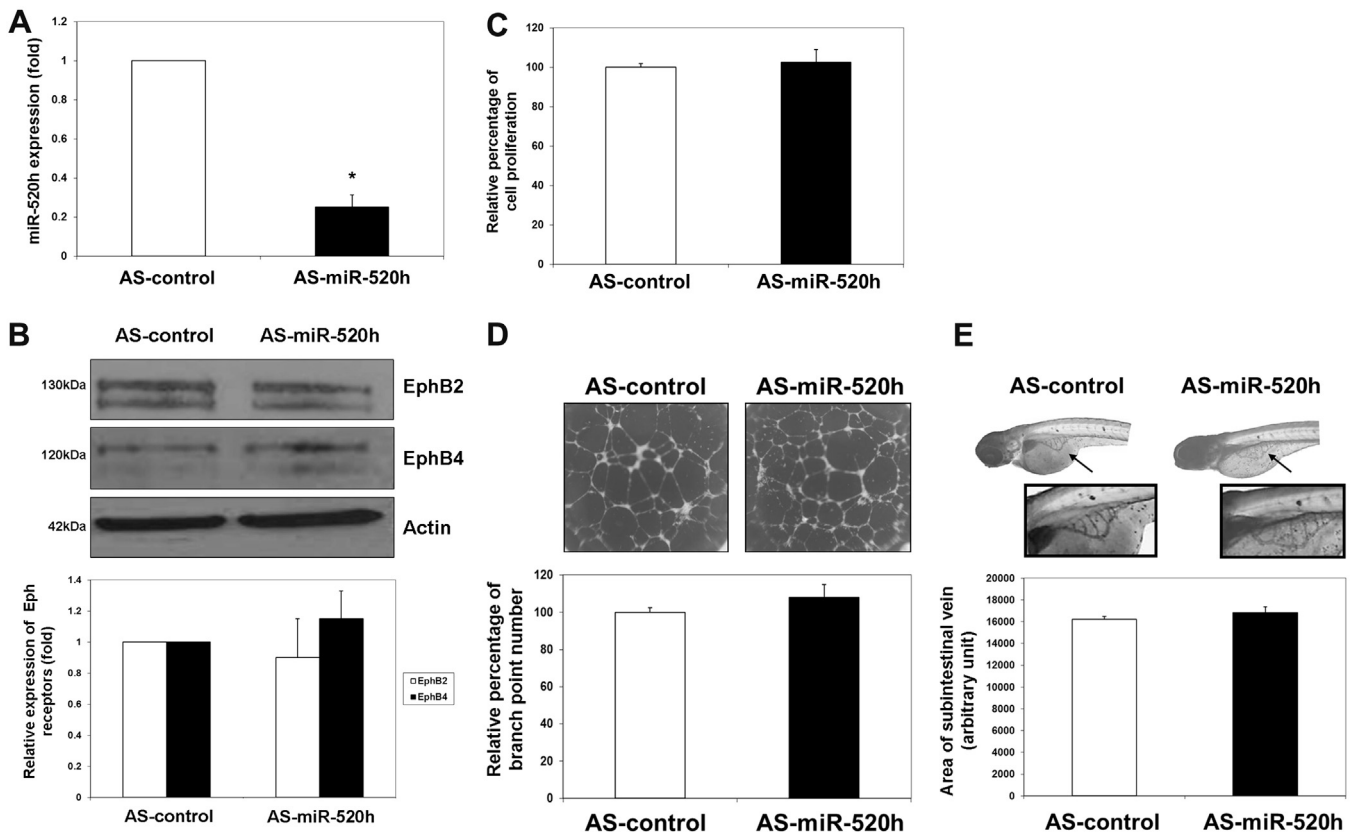


Fig. 6. Reduced level of the mature hsa-miR-520h (miR-520h) exhibits no effects on ephrin receptor (Eph) B2 and EphB4 expression, human-umbilical-vein-endothelial-cell (HUVEC) proliferation and tubulogenesis, and zebra-fish subintestinal-vessel (SIV) formation. (A) Transfection of AS-miR-520h oligonucleotide (20nM) for 24 h effectively reduced the miR-520h level in HUVECs. The miR-520h level was quantitated by quantitative real-time polymerase chain reaction. Three independent experiments were performed, and each experiment was in three replicates. (B) Decreased level of miR-520h exhibits no significant effect on EphB2 and EphB4 expressions in HUVECs. Total protein was harvested from AS-miR-520h or AS-control transfected HUVECs, and EphB2 and EphB4 expression levels were measured by Western blotting (upper panel), and quantified with actin normalization (lower panel). (C) and (D) Transfection of AS-miR-520h oligonucleotide exerts no effect on HUVEC proliferation and tubulogenesis. After transfection, HUVECs were cultured for 48 h, and growth inhibition was determined by 3-(4,5-Dimethylthiazol-2-yl)-2,5-Diphenyltetrazolium Bromide (MTT) assay. Tubulogenesis was measured by counting the number of branch points formed by HUVECs on the Matrigel. Three independent experiments were performed, and each experiment was in four replicates. (E) Microinjection of AS-miR-520h into zebra-fish embryo has no effect on the SIV basket formation. Photomicrographs depict SIV formation in 3 days postfertilization fish embryo in defined condition. The area of the SIV basket was measured by ImageJ software. Values are presented as means \pm standard deviation. Asterisks denote a significant difference compared with the values for the corresponding control. * $p < 0.05$, ** $p < 0.01$, *** $p < 0.001$.

colonization model [20,21]. Wang et al [22] also demonstrated that miR-520h could act as a potent suppressor of pancreatic cancer cell (PANC-1) migration and invasion via the down-regulation of breast-cancer-resistance-protein (ABCG2) expression. Obviously, miR-520h is most likely to mediate cell motility; therefore, we believed that Rg3-induced miR-520h would also play a critical role in modulating endothelial-cell motility and resulted in angiosuppression. According to the computational-prediction analysis, among the target proteins of miR-520h, EphB2 and EphB4 were the most relevant candidates. Indeed, our data showed that Rg3-induced overexpression of miR-520h resulted in the reduction of EphB2 and EphB4 proteins. Actually, the Eph family is the largest receptor-tyrosine-kinase family; the activation of Eph receptor by their membrane-anchored ligands (ephrins) (Eph-ephrin interaction) mediates the critical steps of angiogenesis and vascular-network formation, including endothelial cell-to-endothelial/surrounding-mesenchymal-cell interactions, cell adhesion to extracellular matrix, and cell migration [23–25]. Moreover, it has been shown that ephrin-B ligand and Eph-B receptor induced angiogenic sprouting by stimulating reverse and forward signaling [26]. Besides, as the downstream signaling of EphB4 includes the key pathway of angiogenesis, such as phosphatidylinositol-3-kinase/Akt/endothelial nitric oxide synthase/protein kinase

G/mitogen-activated-protein-kinase cascade, and matrix metallo proteinase-2 and -9 production [27], it implicated that suppression of Ephs could significantly interrupt a lot of cellular activities, including cell proliferation and migration. Indeed, this inhibitory pathway would be one of the angiosuppressive mechanisms of Rg3.

However, a recent finding proposed that Eph/ephrin signaling mechanism might also correlate with VEGF-induced angiogenesis and VEGFR function in developmental and tumor angiogenesis [28,29]. As suggested by Sawamiphak et al [30], the Eph/ephrin signaling at the tip-cell filopodia could regulate the proper spatial activation of VEGFR-2 endocytosis, and signaling to direct the filopodial extension. Subsequently, it could control the vascular morphogenesis and sprouting angiogenesis [30]. Meanwhile, the internalization of VEGFR-2 and -3 was found to depend on Eph/ephrin signaling [31,32], whereas we have also found that Rg3 could suppress VEGFR-2 production in HUVECs (data not shown). This implicated that the Rg3-induced down-regulation of EphB2 and EphB4 in endothelial cells (receptor-expressing cells) might suppress the reverse-signaling pathway of the adjacent ephrin-ligand-expressing cells (including tumor and endothelial cells), and resulted in the inhibition of VEGFR-2 expression and subsequent VEGF signaling that lead to angiosuppression.

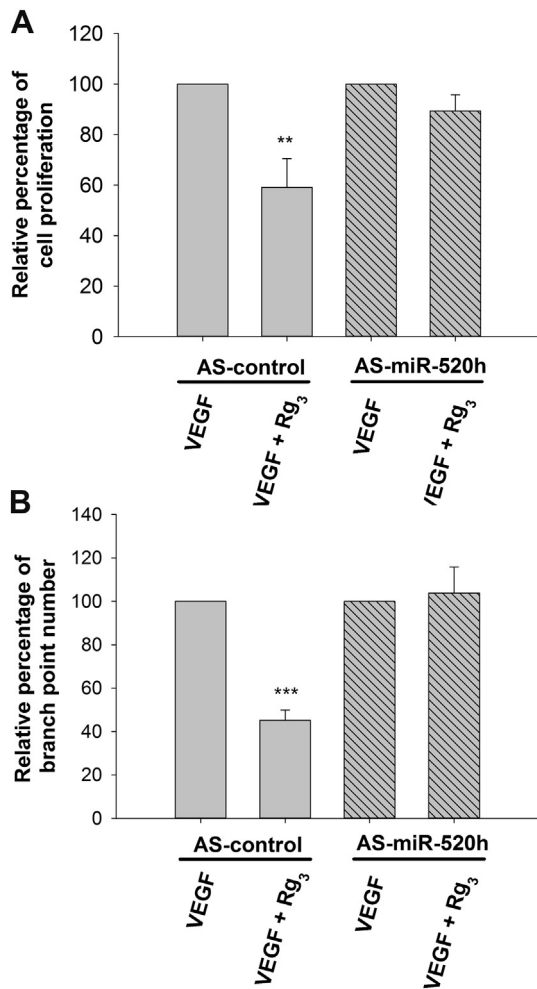


Fig. 7. Decreased level of the mature hsa-miR-520h (miR-520h) abolishes the angiostimulatory effects of 20(R)-ginsenoside-Rg3 (Rg3) on human-umbilical-vein endothelial cells (HUVECs). HUVECs were transfected with AS-control or AS-miR-520h oligonucleotide (20nM) for 24 h, followed by treatment with vascular endothelial growth factor (VEGF) alone or VEGF + Rg3. (A) After Rg3 treatment, HUVECs were cultured for 48 h, and cell proliferation was determined by 3-(4,5-Dimethylthiazol-2-yl)-2,5-Diphenyltetrazolium Bromide (MTT) assay. (B) Tubulogenesis was measured by counting the number of branch points formed by HUVECs on the Matrigel. Three independent experiments were performed, and each experiment was in four replicates. Values are presented as means \pm standard deviation. Asterisk denotes a significant difference compared with the values for the corresponding control. ** $p < 0.01$, *** $p < 0.001$.

In recent years, the therapeutic potential and pharmacological mechanisms of natural phytochemicals have been of great interest. Ginsenoside is one of the pharmacological active compounds that have been studied in detail for their diverse effects [33–36].

5. Conclusion

In this study, we demonstrated that Rg3-induced angiostimulation could be mediated by miR-520h, whereas miR-520h is proposed to negatively regulate angiogenesis through suppressing EphB2 and EphB4 expressions, as shown in the inhibition of proliferation and tubulogenesis of HUVECs, and the SIV formation of zebra fish. These findings further supplement the lack of information on the angiostimulatory mechanism of Rg3. Furthermore, the regulations of Eph/ephrin molecules and miRNAs have been reported as molecular targets for therapeutic approaches; this implicates a great potential for developing Rg3 as a potent angiostimulatory agent.

Conflict of interest statement

None.

Acknowledgments

This work was supported by the General Research Fund (HKBU 261810) of the Research Grant Committee, Hong Kong SAR Government and Dr. Gilbert Hung Ginseng Laboratory Fund.

References

- Chen J, Peng H, Ou-Yang X, He X. Research on the antitumor effect of ginsenoside Rg3 in B16 melanoma cells. *Melanoma Res* 2008;18:322–9.
- Mochizuki M, Yoo YC, Matsuzawa K, Sato K, Saiki I, Tono-oka S, Samukawa K, Azuma I. Inhibitory effect of tumor metastasis in mice by saponins, ginsenoside-Rb2, 20(R)- and 20(S)-ginsenoside-Rg3, of red ginseng. *Biol Pharm Bull* 1995;18:1197–202.
- Yue PY, Wong DY, Wu PK, Leung PY, Mak NK, Yeung HW, Liu L, Cai Z, Jiang ZH, Fan TP, et al. The angiostimulatory effects of 20(R)-ginsenoside Rg3. *Biochem Pharmacol* 2006;72:437–45.
- Liu TG, Huang Y, Cui DD, Huang XB, Mao SH, Ji LL, Song HB, Yi C. Inhibitory effect of ginsenoside Rg3 combined with gemcitabine on angiogenesis and growth of lung cancer in mice. *BMC Cancer* 2009;9:1471–2407.
- Zhang Q, Kang X, Yang B, Wang J, Yang F. Antiangiogenic effect of capecitabine combined with ginsenoside Rg3 on breast cancer in mice. *Cancer Biother Radiopharm* 2008;23:647–53.
- Xu TM, Xin Y, Cui MH, Jiang X, Gu LP. Inhibitory effect of ginsenoside Rg3 combined with cyclophosphamide on growth and angiogenesis of ovarian cancer. *Chin Med J (Engl)* 2007;120:584–8.
- Huang X, Hou M, Yi C, Song H. Anti-angiogenic effects of low-dose gemcitabine combined with ginsenoside Rg3 on mouse Lewis lung carcinoma. *Zhongguo Fei Ai Za Zhi* 2006;9:132–6 [Chinese].
- Kang XM, Zhang QY, Tong DD, Zhao W. Experimental study on anti-angiogenesis in mice with Lewis lung carcinoma by low-dose of cyclophosphamide combined with ginsenoside Rg3. *Zhongguo Zhong Xi Yi Jie He Za Zhi* 2005;25:730–3 [Chinese].
- Chen MW, Ma AQ, Ni L, Huang C, Zhang DZ, Niu XY. Effect of ginsenoside on the cellular proliferation, apoptosis and cell cycles in LC A549 and HUVEC 304 cell lines. *Zhong Nan Da Xue Xue Bao Yi Xue Ban* 2005;30:149–52 [Chinese].
- Bartel DP. MicroRNAs: genomics, biogenesis, mechanism, and function. *Cell* 2004;116:281–97.
- Kim VN, Nam JW. Genomics of microRNA. *Trends Genet* 2006;22:165–73.
- Ambros V. The functions of animal microRNAs. *Nature* 2004;431:350–5.
- Erson AE, Petty EM. MicroRNAs in development and disease. *Clin Genet* 2008;74:296–306.
- Chan LS, Yue PY, Mak NK, Wong RN. Role of microRNA-214 in ginsenoside-Rg1-induced angiogenesis. *Eur J Pharm Sci* 2009;38:370–7.
- Chan LS, Yue PY, Wong YY, Wong RN. MicroRNA-15b contributes to ginsenoside-Rg1-induced angiogenesis through increased expression of VEGFR-2. *Biochem Pharmacol* 2013;86:392–400.
- Chan YK, Kwok HH, Chan LS, Leung KS, Shi J, Mak NK, Wong RN, Yue PY. An indirubin derivative, E804, exhibits potent angiostimulatory activity. *Biochem Pharmacol* 2012;83:598–607.
- Nagpal M, Nagpal K, Nagpal PN. A comparative debate on the various anti-vascular endothelial growth factor drugs: pegaptanib sodium (Macugen), ranibizumab (Lucentis) and bevacizumab (Avastin). *Indian J Ophthalmol* 2007;55:437–9.
- Scapoli L, Palmieri A, Lo Muzio L, Pezzetti F, Rubini C, Girardi A, Farinella F, Mazzotta M, Carinci F. MicroRNA expression profiling of oral carcinoma identifies new markers of tumor progression. *Int J Immunopathol Pharmacol* 2010;23:1229–34.
- Hromadnikova I, Kotlabova K, Jirasek JE, Doucha J. Detection of placenta-specific microRNAs in maternal circulation. *Ceska Gynekol* 2010;75:252–6 [Czech].
- Su JL, Chen PB, Chen YH, Chen SC, Chang YW, Jan YH, Cheng X, Hsiao M, Hung MC. Downregulation of microRNA miR-520h by E1A contributes to anticancer activity. *Cancer Res* 2010;70:5096–108.
- Yu YH, Chen HA, Chen PS, Cheng YJ, Hsu WH, Chang YW, Chen YH, Jan Y, Hsiao M, Chang TY, et al. MiR-520h-mediated FOXO2 regulation is critical for inhibition of lung cancer progression by resveratrol. *Oncogene* 2013;32:431–43.
- Wang F, Xue X, Wei J, An Y, Yao J, Cai H, Wu J, Dai C, Qian Z, Xu Z, et al. hsa-miR-520h downregulates ABCG2 in pancreatic cancer cells to inhibit migration, invasion, and side populations. *Br J Cancer* 2010;103:567–74.
- Cheng N, Brantley DM, Chen J. The ephrins and Eph receptors in angiogenesis. *Cytokine Growth Factor Rev* 2002;13:75–85.
- Zhang J, Hughes S. Role of the ephrin and Eph receptor tyrosine kinase families in angiogenesis and development of the cardiovascular system. *J Pathol* 2006;208:453–61.

- [25] Salucci O, Tosato G. Essential roles of EphB receptors and EphrinB ligands in endothelial cell function and angiogenesis. *Adv Cancer Res* 2012;114:21–57.
- [26] Adams RH, Wilkinson GA, Weiss C, Diella F, Gale NW, Deutsch U, Risau W, Klein R. Roles of ephrinB ligands and EphB receptors in cardiovascular development: demarcation of arterial/venous domains, vascular morphogenesis, and sprouting angiogenesis. *Genes Dev* 1999;13:295–306.
- [27] Steinle JJ, Meininger CJ, Forough R, Wu G, Wu MH, Granger HJ. Eph B4 receptor signaling mediates endothelial cell migration and proliferation via the phosphatidylinositol 3-kinase pathway. *J Biol Chem* 2002;277:43830–5.
- [28] Heroult M, Schaffner F, Augustin HG. Eph receptor and ephrin ligand-mediated interactions during angiogenesis and tumor progression. *Exp Cell Res* 2006;312:642–50.
- [29] Kuijper S, Turner CJ, Adams RH. Regulation of angiogenesis by Eph–ephrin interactions. *Trends Cardiovasc Med* 2007;17:145–51.
- [30] Sawamiphak S, Seidel S, Essmann CL, Wilkinson GA, Pitulescu ME, Acker T, Acker-Palmer A. Ephrin-B2 regulates VEGFR2 function in developmental and tumour angiogenesis. *Nature* 2010;465:487–91.
- [31] Wang Y, Nakayama M, Pitulescu ME, Schmidt TS, Bochenek ML, Sakakibara A, Adams S, Davy A, Deutsch U, Lüthi U, et al. Ephrin-B2 controls VEGF-induced angiogenesis and lymphangiogenesis. *Nature* 2010;465:483–6.
- [32] Horowitz A, Seerapu HR. Regulation of VEGF signaling by membrane traffic. *Cell Signal* 2012;24:1810–20.
- [33] Yue PY, Wong DY, Ha WY, Fung MC, Mak NK, Yeung HW, Leung HW, Chan K, Liu L, Fan TP, et al. Elucidation of the mechanisms underlying the angiogenic effects of ginsenoside Rg(1) *in vivo* and *in vitro*. *Angiogenesis* 2005;8:205–16.
- [34] Chan LS, Yue P, Kok TW, Keung MH, Mak NK, Wong R. Ginsenoside-Rb1 promotes adipogenesis through regulation of PPAR γ and microRNA-27b. *Horm Metab Res* 2012;44:819–24.
- [35] Kwok HH, Yue PYK, Mak NK, Wong RNS. Ginsenoside Rb1 induces type I collagen expression through peroxisome proliferator-activated receptor-delta. *Biochem Pharmacol* 2012;84:532–9.
- [36] Kwok HH, Guo GL, Lau JKC, Cheng YK, Wang JR, Jiang ZH, Keung MH, Mak NK, Yue PY, Wong RN. Stereoisomers ginsenosides-20(S)-Rg₃ and -20(R)-Rg₃ differentially induce angiogenesis through peroxisome proliferator-activated receptor-gamma. *Biochem Pharmacol* 2012;83:893–902.